

Tegaserod Maleate Exerts Anti-Tumor Effects on Prostate Cancer Via Repressing Sonic Hedgehog Signaling Pathway

Maoping Cai^{1,2,3}, Yaying Hong⁴, Songyu Li², Jiading Guo^{1,3}, Yang-Zi Ren⁵, Mingkun Chen¹, Yuan Liu⁴, Zhe-Sheng Chen⁶, Ninghan Feng^{7,8,9,*}, Zhanghui Chen^{2,*} and Shan-Chao Zhao^{1,3,4,10,*}

¹Department of Urology, The Third Affiliated Hospital of Southern Medical University, Guangzhou, 510630, Guangdong, PR China

²Zhanjiang Institute of Clinical Medicine, Central People's Hospital of Zhanjiang, Zhanjiang, 524045, Guangdong, PR China

³The Third Clinical college, Southern Medical University, Guangzhou, 510630, Guangdong, PR, China

⁴Department of Urology, Nanfang Hospital, Southern Medical University, Guangzhou, 510515, Guangdong, PR China

⁵Department of Oncology, The First Affiliated Hospital of Guangzhou University of Chinese Medicine, Guangzhou, 510405, Guangdong, PR China

⁶Department of Pharmaceutical Sciences, College of Pharmacy and Health Sciences, St. John's University, Queens, NY 11439, United States of America

⁷Department of Urology, Jiangnan University Medical Center, Wuxi, 214002, PR China

⁸Wuxi School of Medicine, Jiangnan University, Wuxi, 214002, PR China

⁹Department of Urology, Affiliated Wuxi No.2 Hospital, Nanjing Medical University, Wuxi, 214002, PR China

¹⁰Department of Urology, The Fifth Affiliated Hospital of Southern Medical University, Guangzhou, 510920, Guangdong, PR China

***Corresponding Authors:** Shan-Chao Zhao, Department of urology, The Third Affiliated Hospital of Southern Medical University, Guangzhou, 510630, Guangdong, PR China, Tel: +8613794399828, E-mail: lulululu@smu.edu.cn

Zhanghui Chen, Zhanjiang Institute of Clinical Medicine, Central People's Hospital of Zhanjiang, Zhanjiang, 524045, Guangdong, PR China, Tel: +8613634133457, Email: zjcell@126.com

Ning-Han Feng, Department of Urology, Jiangnan University Medical Center, Wuxi, 214002, PR China, Tel: +86510-68563005, Fax: 86510-68562051, E-mail: fnh888@njmu.edu.cn

Citation: Maoping Cai, Yaying Hong, Songyu Li, Jiading Guo, Yang-Zi Ren et al. (2024) Tegaserod Maleate Exerts Anti-Tumor Effects on Prostate Cancer Via Repressing Sonic Hedgehog Signaling Pathway, SAJ Cancer Sci 10: 101

Abstract

Prostate cancer (PCa) is a highly common type of malignancies and affects millions of men in the world since it is easy to recur or emerge therapy resistance. Therefore, it is urgent to find novel treatments for PCa patients. In the current study, we found that tegaserod maleate (TM), an FDA-approved agent, inhibits the proliferation, colony formation, migration as well as invasion, causes the arrest of cell cycle and promotes apoptosis of PCa cells in vitro. In addition, TM suppresses the tumor growth in the cell-derived xenograft (CDX) mouse model in vivo. Mechanistically, TM exerts anti-cancer effect via downregulating GLI2, its target and inhibiting sonic hedgehog (SHH) signaling. In brief, our findings demonstrate that TM effectively inhibits the activities of PCa through SHH pathway and provide a potential new agent for the treatment of PCa.

Keywords: Prostate cancer (PCa); Tegaserod maleate (TM); Sonic hedgehog (SHH) signaling; GLI2; Treatment

Introduction

Prostate cancer (PCa) is the most prevalent type of male malignancies and the main cause of cancer-related death among males globally [1-3]. Regardless of initial susceptibility to androgen deprivation therapy (ADT), the majority of patients eventually develop to castration-resistant prostate cancer (CRPC) within 18-36 months on ADT [4, 5]. With advancements of medical technologies, various treatments such as chemical, endocrine, immune and radical therapies for PCa have been developed [6, 7]. However, these treatments often lead to therapy resistance, resulting in low cure rates and poor prognosis [8, 9]. Therefore, there is an urgent need to explore novel strategies, and anti-cancer mechanisms to enhance treatment efficacy and provide new options for the management of PCa, particularly CRPC. Tegaserod maleate (TM) is a drug that selectively acts as a partial agonist on the 5-HT₄ receptor and an antagonist on the 5-HT_{2B} receptor. It has been clinically used for several decades in the treatment for patients with irritable bowel syndrome (IBS) due to its effects in the gastrointestinal (GI) tract [10]. In recent years, researchers found a novel potential role of TM as an anti-cancer drug. Multiple studies have demonstrated that TM strongly inhibits the development of numerous malignancies, including acute myeloid leukemia, melanoma, breast cancer and gastric cancer [11-15]. Recently, studies have found that YTHDF1, an m⁶A reader protein, is overexpressed in PCa and plays an essential role in the progression as well as therapy resistance in PCa [16, 17]. Dr Hong and colleagues identified TM as a potent YTHDF1 inhibitor [11]. Consequently, we speculate TM exerts profound inhibitory effects on PCa and verify it. In this study, we identified TM as a potent drug to suppress PCa. TM efficiently represses PCa cell proliferation, migration, and invasion while also promoting apoptosis. Transcriptomic and functional analyses revealed that TM led to the decrease of GLI2 and its target genes, thus inhibiting the sonic hedgehog (SHH) signaling pathway. Hedgehog (HH) proteins, which include SHH, desert hedgehog (DHH), and indian hedgehog (IHH), from *Drosophila* to humans, play critical roles in the evolution of organs and cells [18]. HH binding to the patched receptor (PTC) in vertebrates reduces the inhibition of the co-receptor smoothed (SMO), activating downstream GLI transcription factors such as GLI1, GLI2, and GLI3. GLI1 is a transcriptional activator, while GLI2 and GLI3 comprise both activator and repressor forms [19]. GLI3 undergoes proteolytic cleavage to provide GLI3R, a C-terminally truncated repressor form in the absence of HH, while GLI2 is targeted for inhibition. When HH is present, GLI3 cleavage into GLI3R is prevented by the ensuing signaling, which also stabilizes GLI2, allowing it to subsequently be N-terminally truncated into its activator form (GLI2A) [20]. Generally, HH has a conserved effect of changing GLIs from repressors to activators, enabling coordinated transcriptional activities [19]. In addition, SHH plays an essential role in the development of cancers including PCa [21]. Above all, we speculate that TM may serve as a potential new antagonist of SHH signaling pathway, and be used to treat diseases caused by the activation of SHH signaling. In our study, we identified TM as a potent drug to suppress PCa. It efficiently inhibits PCa cell proliferation, migration, invasion, and induces apoptosis *in vitro*. It also inhibits tumor development *in vivo*. Transcriptomic and functional analyses revealed that TM treatment led to the decrease of GLI2 and inhibition of the SHH signaling pathways, accounting for its underlying mechanism of its antitumor activity.

Material and Methods

Cell Culture and Treatment

The ATCC (Manassas, VA, USA) provided the DU145, PC-3, LNCaP, 22RV-1, and RWPE-1 cell lines, which were then cultivated in accordance with earlier instructions [22-24]. Prior to being used, cell lines were verified to be mycoplasma-free by short tandem repeat (STR) profiling. We did not employ cells that were beyond passage 20. Cells in experimental cultures were exposed to the TM doses listed (MCE, HY-14153A). Dimethyl sulfoxide (Sigma, S-002-M) was used as the vehicle for TM.

Cell Proliferation Assay

3000 cells per well were seeded into 96-well plates with 100 μ L of medium containing various experimental drug concentrations at 37°C for the appropriate number of hours. The medium was then replaced with 100 μ L of a solution containing 10 μ L from the Cell Counting Kit (CCK-8; MCE and HY-K0301), and the plates were incubated for an additional two hours at 37°C and 5% CO₂.

Ultimately, a Thermo microplate reader was used to measure the OD value at 450 nm. In order to conduct the colony formation experiments, 1500 cells per well were seeded onto 6-well plates, and the cells were grown at 37°C for 12 days using varying concentrations of TM as the vehicle. Finally, the cells were photographed, dyed with crystal violet, and preserved in 4% paraformaldehyde (PFA).

Flow Cytometry Analysis

Using the Cell Cycle Staining Kit (KeyGEN, KGA512) and the associated procedure, the cell cycle analysis was carried out. In short, after 48 hours of growth in 6-well plates (106 cells/well) with either vehicle or TM, the cells were collected for propidium iodide (PI) staining. The cells were ultimately examined using a BD Biosciences C6 flow cytometer. The apoptosis test was carried out in accordance with the relevant protocol using the Annexin V- PE/7-AAD Staining Kit (KeyGEN, KGA1018). In 6-well plates (106 cells/well), cells were grown with vehicle or TM for 48 hours at 37°C. Following that, the cells were collected and preserved for the night at 4°C in 70% ethanol. Following the manufacturer's directions, cells were collected for 7-Aminoactinomycin D (7-AAD) after the ethanol was removed. The cells were ultimately examined using a BD Biosciences C6 flow cytometer.

Scratch Assays and Transwell Experiments

Ibidi Culture-Insert (Ibidi GmbH, Munich, Germany) was used to set up the scratch assay. Cells were seeded into the culture-insert in 12-well plates. To reduce cell growth after the attachment of the cells, the culture-insert was taken out and the culture medium was substituted with media containing vehicle or TM containing 1% fetal bovine serum (FBS). Lastly, a light microscope was used to inspect and take pictures of the scratch after 0, 12, and 24 hours. ImageJ was used to quantify cell movement.

Regarding the transwell migration experiment, 100 µL of media devoid of FBS was used to seed 4×10^4 cells into the top chamber of 24-well transwell plates (6.5 mm insert, 8.0 µm pores). To the bottom compartment, 600 µL of 10% FBS-supplemented media was introduced. A cotton swab was used to gently remove the cells off the chamber's top surface after a 24-hour period. After that, the migrating cells on the chamber bottom were stained with crystal violet and preserved with 4% PFA.

As to the transwell invasion studies, 24 well transwell plates were filled with an upper chamber containing 100 µL of diluted Matrigel (BD), which was then incubated for two hours at 37°C with 5% CO₂. 100 µL of serum-free media was used to seed about 4×10^4 cells into the top chamber. To the bottom compartment, 600 µL of 10% FBS-supplemented media was introduced. Using a cotton-tipped swab, the Matrigel and non-invading cells were carefully removed from the chamber's top surface after a 24-hour period. After that, the cells on the chamber bottom were fixed and dyed so they could be seen. For quantification, three randomly chosen fields from each chamber were photographed under a light microscope.

Plasmid Construction and Transfection

Plasmid construction and transfection was performed as stated previously [25]. The pCDH vector's NheI and EcoRI restriction sites were subcloned with the full-length coding sequences (CDS) of GLI2. DNA sequencing served as validation for each plasmid. As directed by the manufacturer, Lipofectamine 3000 (Invitrogen Life Technologies®, Carlsbad, CA, USA) was used to transfect plasmids. GLI2 expression was assessed by Western blotting using anti-GLI2 (Abclonal, A16863) antibodies and RT-qPCR.

RNA Isolation, RNA-Seq, RT-Qpcr and Western Blotting

The methods previously described [11] were followed for RNA isolation, RNA-seq, real-time quantitative polymerase chain reaction (RT-qPCR), and Western blotting. TRIzol Reagent (Invitrogen) was used to extract total RNA from PCa cells treated with vehicle or TM for 48 hours, and RNA seq analysis was performed by Hangzhou Kaitai Biotechnology Co., Ltd. (Hangzhou, China).

Using the Evo M-MLV kit (AG11606), 1 µg of RNA was transcriptionally converted to complementary DNA (cDNA) for RT-

qPCR. SYBR Green reaction mix (AG11732) and a Light Cycler 96 System (Roche, Basel, Switzerland) were used for the qPCR. Ct, the cycle threshold, was used to compute the relative expression using the $2^{-\Delta\Delta Ct}$ method. Supplementary Table 1 contains a list of sequences of all the particular primers.

About Western blotting, the protease inhibitor cocktail-containing RIPA Lysis and Extraction Buffer (Fudebio, FD008) was used to lyse the cells. After that, proteins were separated by SDS-polyacrylamide gel electrophoresis and put onto membranes made of nitrocellulose. The membranes were blocked for 1 hour at 25°C with 5% fat-free milk, and then they were treated with primary antibodies for an overnight period at 4°C: GLI2 antibody (Abclonal, A16863), PTCH1 antibody (Abclonal, A0826), SUFU antibody (Abclonal, A13429), SMO antibody (Abclonal, A3274), SHH antibody (Abclonal, A18863), Cyclin D1 antibody (Abclonal, A11022), Cyclin D2 antibody (Abclonal, A1773), Cyclin E1 antibody (Abclonal, A22461), CDK4 antibody (Abclonal, A2352), GLI1 antibody (Abclonal, A14675), c-Myc antibody (Abclonal, A1309), Bcl-2 antibody (Abclonal, A0208), GAPDH antibody (CST, #2118), β -actin antibody (CST, #4970) and β -tubulin antibody (CST, #2146). The membranes were then incubated with HRP-conjugated, anti-rabbit secondary antibody (Sigma, GENA934) 1 hour at room temperature.

Mouse Model and In Vivo Treatments

The animal care committee of the Central People's Hospital in Zhanjiang authorized the animal research. Subcutaneous injections of 1×10^6 DU145 or PC-3 cells were given to male athymic nude mice (Jiangsu JICUI Laboratory Animal) that were five weeks old. Mice were injected intraperitoneally with vehicle or TM (2.5 mg/kg) every two days for seven days after implantation.

PEG 300 and Tween-80 were used as the TM solvents for the in vivo investigation. Following medication delivery, the tumor volume and body weight of nude mice were monitored every two days for the following three weeks. The formula $V = L \times W^2/2$ (V = volume, mm³; L = major axis length, mm; W = minor axis length, mm) was used to estimate the tumor volume. Using a digital caliper, the lengths of the main and minor axes were measured. Following a three-week period of medication treatment, the tumors were removed, quantified, captured on film, embedded in 4% PFA, and sectioned into paraffin.

Immunohistochemistry Assays

We used the paraffin slices of the xenograft tumor for immunohistochemistry (IHC). The following tools were used for IHC: HRP-conjugated goat anti-rabbit IgG (Fudebio, FDR007), GLI2 antibody (Abclonal, A16863), cleaved caspase-3 antibody (CST, 9661), Ki67 antibody (CST, #9027), SHH antibody (Abclonal, A18863) and Instant Immunohistochemistry Kit I (KeyGEN, KGOS300). Under a light microscope, stained slices were viewed and captured on camera.

Statistical Analysis

Software for graphics was GraphPad Prism 9, and statistical analysis was done using SPSS. The mean \pm SD was used to represent the experimental outcomes. For statistical analysis, the student's t test was used. P-values less than 0.05 (*), less than 0.01 (**), or less than 0.001 (***) were regarded as statistically significant.

Results

TM Inhibits the Proliferation and Promotes Apoptosis of Pca Cells in Vitro

To investigate whether TM inhibits PCa cell growth, we first performed CCK-8 assay on PCa cells including DU145, PC-3, 22RV-1, LNCaP and normal epithelial cell (RWPE-1), treated with TM to detect their viability. The findings demonstrated that although TM had little impact on RWPE-1, it dramatically suppressed the growth of all PCa cells (Figure 1A). TM exerted an apparent influence in androgen-independent PCa cells (DU145 and PC-3) in both a dose-dependent and time-dependent manner (Figure 1B-C). We used these two cell lines to carry out a series of follow-up investigations. Additionally, we also observed TM obvi-

ously suppressed the clone formation ability of the PCa cells (Figure 1D-E).

We looked at whether TM would promote PCa cell apoptosis or result in cell cycle arrest as it slowed the development of PCa cells. Using DU145 and PC-3 cells labeled with PI and 7-AAD, we conducted flow cytometric analysis. The results indicated that TM significantly increased the population of G0/G1 cells while reducing the number of cells in S phase or G2/M phase, suggesting a block in the G1/S cell cycle phase (Figure 1F-G). Besides, we found that, in comparison to the vehicle control group, the apoptotic rate of the cells treated with TM was considerably greater (Figure 1H-I). These findings indicate that TM has powerful antitumor effects on PCa cells.

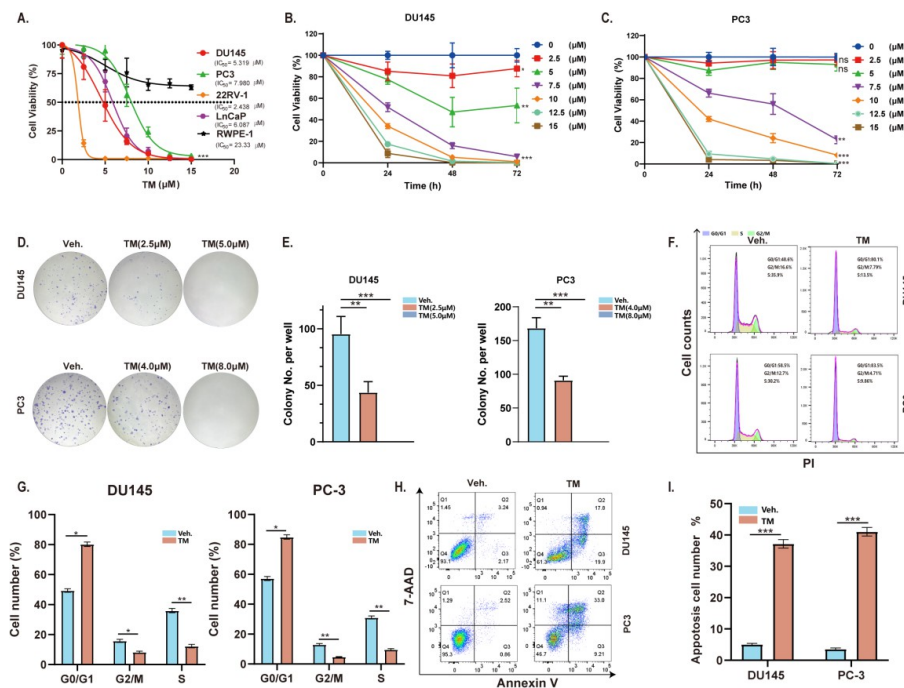


Figure 1: Tegaserod maleate (TM) inhibits proliferation of prostate cancer (Pca) cells.

(A) cells were treated with TM (0, 2.5, 5, 7.5, 10, 12.5, 15 $\mu\text{mol/L}$) for 48 h, and subsequently, cell viability was detected through CCK-8 assays. Statistical analysis was performed between each prostate cancer cell line and RWPE-1. (B and C) DU145 and PC-3 cells were treated with pentamidine (0, 2.5, 5, 7.5, 10, 12.5 and 15 $\mu\text{mol/L}$) for 0, 24, 48 or 72 h, and then, cell viability was determined by CCK-8 assays. Statistical analysis was performed between cells treated with 0 $\mu\text{mol/L}$ TM and each of the other drug concentration groups. (D and E) Colony formation assay on DU145 and PC-3 cells treated with TM (0, 2.5 and 5 $\mu\text{mol/L}$). (F and G) Cell cycle distribution of DU145 and PC-3 cells incubated with 5 $\mu\text{mol/L}$ TM or vehicle for 48 h. (H and I) Flow cytometric assays of the apoptotic percentage (including viable and non-viable apoptotic cells) in TM- and vehicle-treated DU145 and PC-3 cell. Unpaired t test was used for the statistical analysis. * $P < 0.05$; ** $P < 0.01$; *** $P < 0.001$; ns, no significance. Data are presented as mean \pm SD of at least three independent experiments.

TM Represses the Migration and Invasion of Pca Cells in Vitro

To further test whether PCa cells' ability of migration as well as invasion was suppressed by TM, we performed scratch experiment and transwell assays. It was observed that TM treatment significantly reduced the migratory ability of DU145 and PC-3 cells (Figure 2A-B). Additionally, transwell migration tests revealed that TM inhibited cell mobility (Figure 2C-D). We also performed transwell invasion studies to assess the impact of TM on the invasion of PCa cells and observed that the invasion capacity of tumor cells significantly decreased in TM treatment groups compared to vehicle control group as well (Figure 2C-D). These findings suggest that TM effectively inhibits the migration and invasion of PCa cells in vitro.

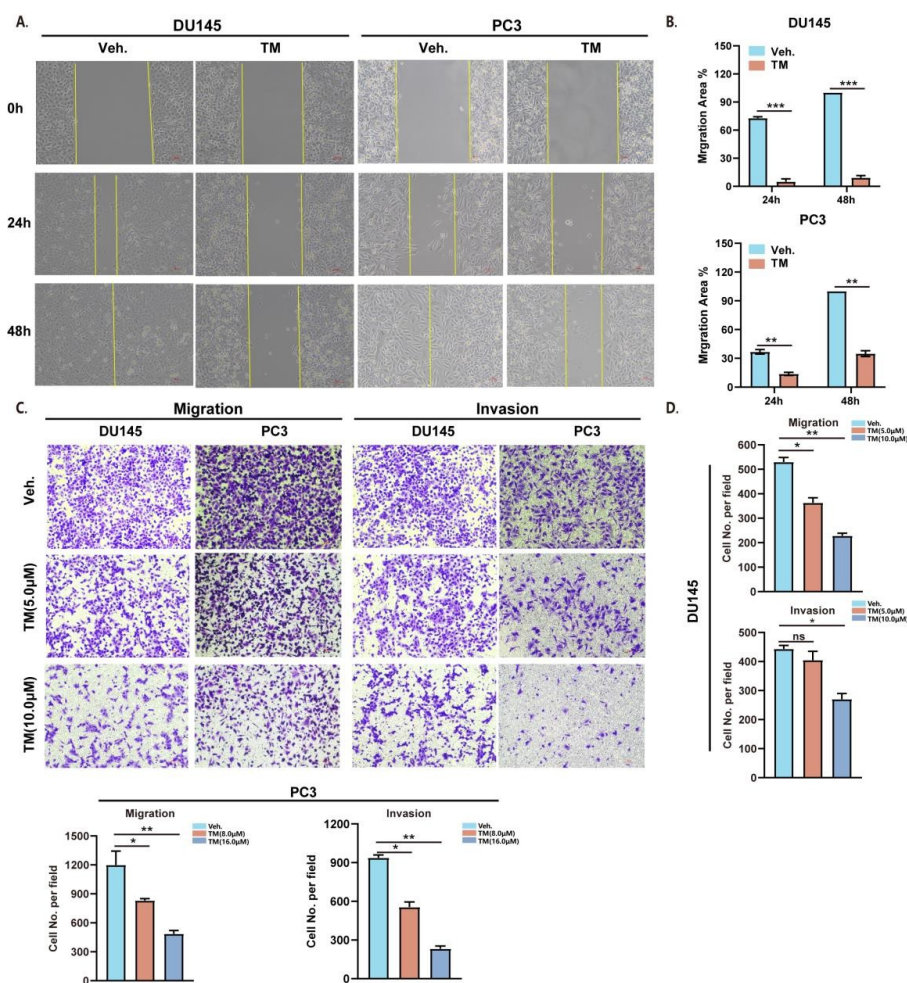


Figure 2: TM suppresses the capacity of migration and invasion in PCa cells

(A and B) Wound- healing assays of DU145 and PC-3 cells treated with 5 $\mu\text{mol/L}$ TM or vehicle. (C and D) Transwell migration and invasion experiments of DU145 and PC-3 cells treated with 5 and 10 $\mu\text{mol/L}$, and 8 and 16 $\mu\text{mol/L}$ TM or vehicle respectively. Unpaired t test was used for the statistical analysis. * $P < 0.05$; ** $P < 0.01$; *** $P < 0.001$; ns, no significance. Data are presented as mean \pm SD of at least three independent experiments.

TM Reduces the Expression of GLI2 and Inhibits SHH Signaling

In order to elucidate the mechanism behind TM's inhibitory effects on PCa cells, we used RNA-seq to assess the transcriptional factors that differed between DU145 and PC-3 cells treated with TM and vehicle. In DU14 and PC-3 cells, we detected 72 and 27 downregulated genes as well as 206 and 227 upregulated genes respectively. Then we focused on the downregulated genes between DU145 and PC-3 cells. After overlap, we obtained three genes, GLI2, RBM14 and TXNIP and performed RT-qPCR to verify their expression. The results were in line with the data from RNA-seq, and we found that GLI2 was the most significantly downregulated gene after TM treatment (Figure 3A-C). Therefore, we listed GLI2 as the candidate gene and detected its protein level. It was found that the protein level of GLI2 in cells treated with TM was reduced significantly (Figure 3D).

As previous reported, GLI2 is a transcription factor, which serves as a crucial role in SHH signaling to mediate the development of cancers [26-29]. Based on this finding, we supposed TM inhibited the activities of PCa cells through SHH pathway and detected the level of SHH related proteins. Interestingly, we observed that the SHH signaling pathway related proteins, including PTCH1, SMO, SUFU, and SHH, decreased apparently both at their mRNA and protein levels (Figure 3 E-F). As GLI2 works by promoting the expression of its target genes consisting of Cyclin D, Cyclin E, Myc and GLI1, we further detected these target genes and the re-

sults demonstrated that the expression of all these genes was reduced (Fig3. G-H). Similarly, we also explored the expression of CDK4, which mediates cell cycle, and Bcl-2, a protein that inhibits apoptosis. The results indicated that the level of these two proteins reduced as well. Taken together, TM could result in the downregulation of GLI2 along with its target genes and inhibit SHH signaling pathway.

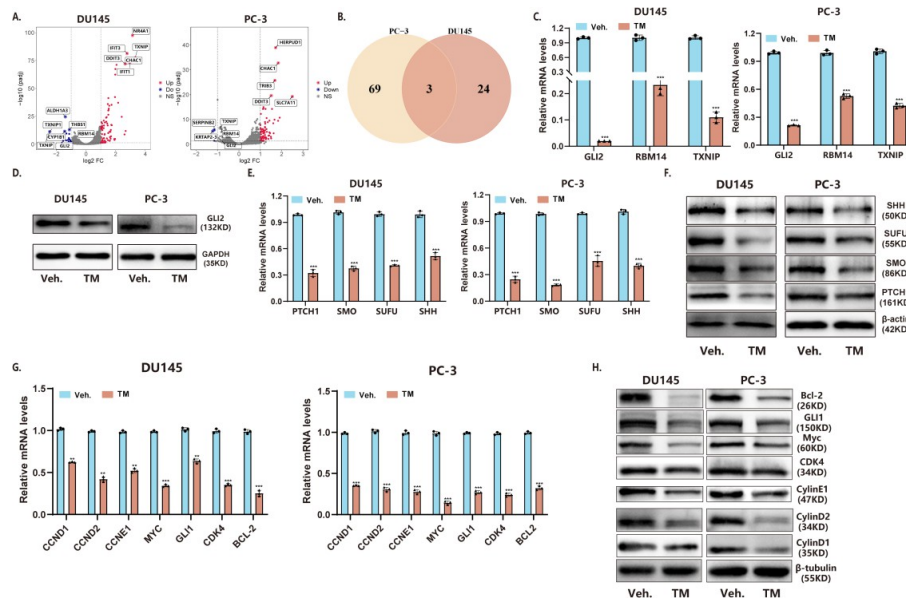


Figure 3: TM represses activities of PCa cells via downregulating GLI2 and its target genes

(A) Scatterplot of RNA-seq data from vehicle and TM treated DU145 and PC-3 cells. The upregulated (red) and downregulated (blue) genes at the translational level are highlighted. (B) The overlap of downregulated genes in DU145 and PC-3 cells. (C) RT-qPCR analysis of transcription levels of the common downregulated genes in DU145 and PC-3 cells. (D) Immunoblot analysis of GLI2 in DU145 and PC-3 cells treated with vehicle and TM. GAPDH was used as a loading control. (E) RT-qPCR analysis of transcription levels and (F) Immunoblot analysis of SHH signaling pathway related proteins in DU145 and PC-3 cells treated with vehicle and TM. β -actin was used as a loading control. (G) RT-qPCR analysis of transcription levels of GLI2 target genes in DU145 and PC-3 cells treated with vehicle and TM. (H) Immunoblot analysis of GLI2 target proteins in DU145 and PC-3 cells treated with vehicle and TM. β -tubulin was used as a loading control. Unpaired t test was used for the statistical analysis. * $P < 0.05$; ** $P < 0.01$; *** $P < 0.001$; ns, no significance. Data are presented as mean \pm SD of at least three independent experiments.

GLI2 Overexpression Alleviates the Effect Caused By TM

To further determine the role GLI2 in TM inhibition of PCa cells, we constructed DU145 (DU145oe) and PC-3 (PC-3oe) cells overexpressing GLI2 through lentivirus while cells infected with vector were selected as the control group (Figure4 A-B). Subsequently, we treated DU145oe and PC-3oe with TM and the results demonstrated TM showed no inhibitory effect on PCa cells overexpressing GLI2 compared to the control group (Figure4 C-I). These findings indicate TM suppresses activities of PCa cells and its target genes through downregulating GLI2.

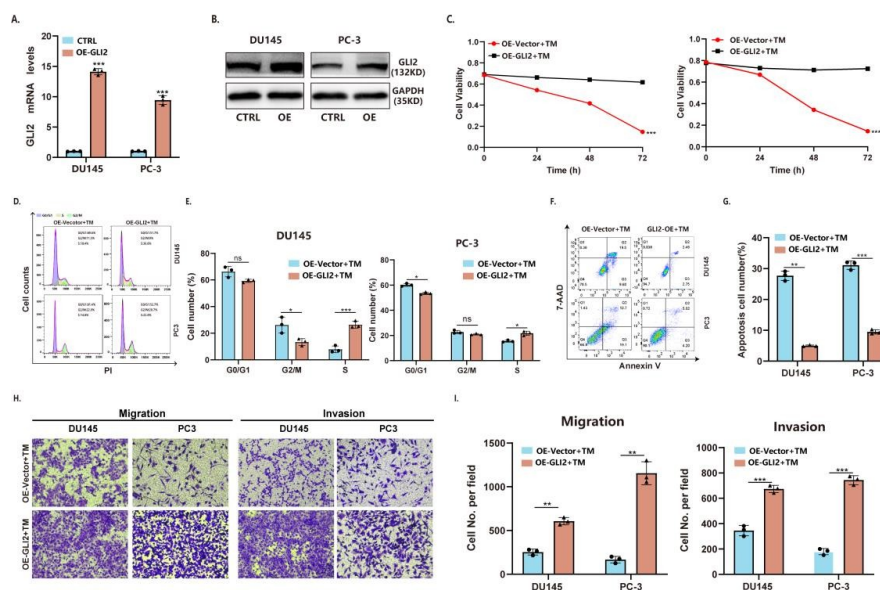


Figure 4: Overexpression of GLI2 reduces the effect induced by TM

(A) RT-qPCR analysis of transcription levels of GLI2 in control and GLI2 overexpressing DU145 and PC-3 cells. (B) Immunoblot analysis of GLI2 in control and GLI2 overexpressing DU145 and PC-3 cells. (C) Cell proliferation analysis in control and GLI2 overexpressing DU145 and PC-3 cells. (D and E) Cell cycle distribution in control and GLI2 overexpressing DU145 and PC-3 cells. (F and G) Flow cytometric assays of the apoptotic percentage (including viable and non-viable apoptotic cells) in control and GLI2 overexpressing DU145 and PC-3 cells. (H and I) Transwell migration and invasion experiments in control and GLI2 overexpressing DU145 and PC-3 cells. Unpaired t test was used for the statistical analysis. * $P < 0.05$; ** $P < 0.01$; *** $P < 0.001$; ns, no significance. Data are presented as mean \pm SD of at least three independent experiments.

TM Suppresses Tumor Growth in Vivo

To investigate whether TM exert an antitumor effect in vivo, we next used a nude mouse xenograft model. TM was discovered to greatly repress the development of xenograft tumors and some of the tumors were even not detectable (Figure 5A-E). In mice given TM, there was no discernible decrease in body weight (Figure 5I). According to IHC experiments, TM treatment increased the percentage of cleaved caspase3 positive cells while decreasing the levels of GLI2, SHH, and Ki67, a proliferating cell marker (Figure 5F-H). These results demonstrate that TM slows the growth of PCa by causing apoptosis and blocking cell division in vivo.

Discussion

In this work, we examine TM's possible anti-cancer properties, a drug once used for the treatment of IBS, but now used as an anti-cancer agent, on PCa cells. Our findings indicate that TM can significantly suppress the proliferation, colony formation, migration, as well as invasion of PCa cells. Moreover, when administered systemically, TM considerably represses the tumor growth ability of PCa in the mouse xenograft model. We also found that TM leads to reduction of GLI2 and inhibits SHH signaling pathway, thus repressing the growth and promoting apoptosis of PCa cells. Developing effective anti-cancer drugs is a challenging task [30-32]. However, repositioning already existing clinical drugs could be an attractive solution, because of their in vivo safety, and pharmacokinetics and pharmacodynamics were well-understood [33]. In this work, the effects of TM on multiple PCa cell lines, including PC-3, LNCaP, DU145, 22RV-1, and RWPE-1 normal prostate epithelial cells were investigated. Interestingly, we found that all cancer cells are sensitive to TM except RWPE-1. Moreover, TM treatment demonstrated great anti-tumor effects on CRPC cells, du145 and PC-3 cells. TM inhibited their proliferation, migration, and invasion, with very little damage to RWPE-1 cells in vitro. In the nude mouse xenograft model, TM showed great anti-tumor effects without causing general toxicity. These findings

suggest that TM could be an encouraging treatment for PCa. Additional researches are required to assess its possible therapeutic use and transfer it into clinical use. RNA-seq analysis shows that after TM treatment, there is an obvious decrease in the transcription levels of GLI2, a transcriptional factor, regulates the cancer cell proliferation and apoptosis in SHH signaling pathway. The SHH signaling pathway is essential to the growth of malignancies. When HH ligand combines with the receptor PTCH1, PTCH1 will be activated and signaling is transferred to downstream molecules including SMO, SUFU/GLI2, thus activating GLI2 and promoting the activated GLI2 into the nucleus. The increased activated GLI2 further accelerates the translation of its target genes. Excitingly, we found that TM could reduce the level of PTCH1 and its downstream proteins, therefore inhibiting SHH signaling pathway (Figure 5 J). The RT-qPCR assays and Western blotting analysis further confirm the decrease in the transcription and translation of GLI2, SHH related proteins and GLI2's target genes. These results suggest that TM may be a potential SHH-targeted PCa treatment drug. Through downregulating GLI2 as well as its target genes, and inhibiting SHH signaling pathway, TM effectively inhibits the growth and promotes apoptosis of PCa cells.

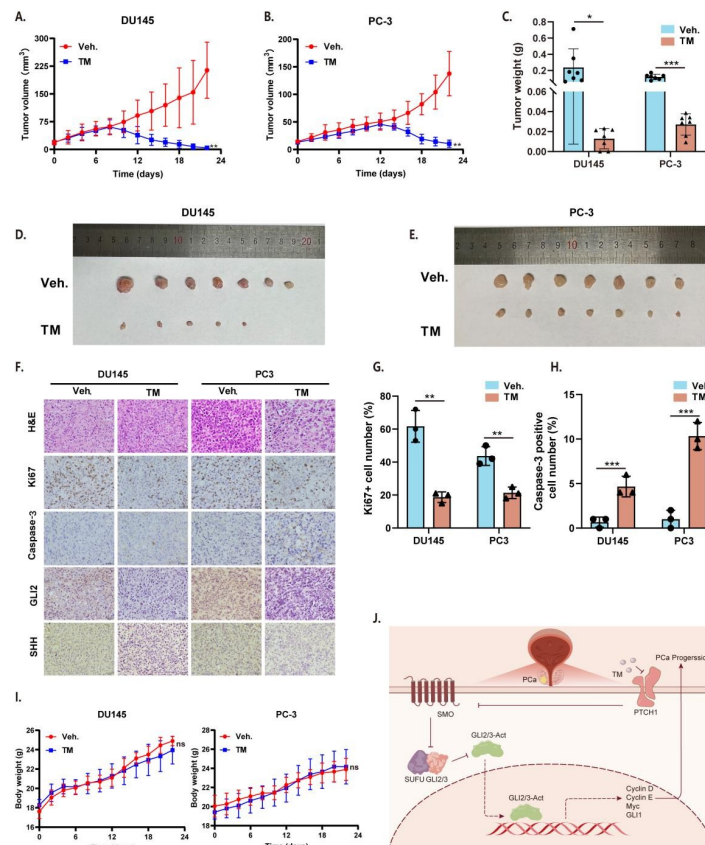


Figure 5: TM inhibits tumor growth in vivo. (A and B) Relative tumor volume in nude mice

Tumor volume was measured once every two days from the day of drug administration. (C) Weight of xenograft tumors when they were harvested. (D and E) Photographs of xenograft tumors when they were harvested. (F) H&E staining and immunohistochemistry images with antibodies against Ki67, cleaved caspase-3, GLI2 and SHH in DU145 and PC-3 xenograft tumors. (G) Proportion of Ki67 positive cells was reduced in xenograft tumors upon TM treatment. (H) Proportion of cleaved caspase-3 positive cells was increased in xenograft tumors upon TM treatment. (I) Body weight of nude mice. Body weight was measured once every two days from the day of drug administration. (J) A schematic model of the mechanism underlying the role of TM in prostate cancer. Unpaired t test was used for the statistical analysis. * $P < 0.05$; ** $P < 0.01$; *** $P < 0.001$. Data are presented as mean \pm SD. As TM could effectively inhibits SHH signaling pathway, TM could be a novel SHH inhibitor and be used to treat diseases caused by the activation of SHH signaling pathway. Future attention could be paid to investigations about this and transfer it into clinical application.

Conclusion

In summary, our study demonstrates that TM could be used to inhibit the progression of PCa. The drug not only suppresses proliferation but also reduces migration as well as invasion in PCa cells. Additionally, TM inhibits the development of tumors in vivo. These findings demonstrate TM's potential as an anti-cancer medication for PCa therapy. TM could be a promising antagonist of SHH signaling pathway, thus being used to treat SHH related diseases.

Appendix A: Supplementary Data

Appendix Table 1: Primer sequence of RT-qPCR

Gene	Forward sequence	Reverse sequence
GLI2	CTGCCTCCGAGAAGCAAGAAG	GCATGGAATGGTGGCAAGAG
RBM14	CCCCGAGCCTCTTATGTGG	GTCATGGGCTGAGTCCGATAG
TXNIP	ATATGGGTGTGTAGACTACTGGG	GCAGGTACTCCGAAGTCTGT
PTCH1	ACTTCAAGGGGTACGAGTATGT	TGCGACACTCTGATGAACCAC
SMO	TCGAATCGCTACCCTGCTG	CAAGCCTCATGGTGCCATCT
SUFU	CACGCCATCTACGGAGAGTG	GTACTTGACGATAGCGGTAACC
SHH	CTCGCTGCTGGTATGCTCG	ATCGCTCGGAGTTTCTGGAGA
CCND1	GCTGCGAAGTGGAACCATC	CCTCCTTCTGCACACATTTGAA
CCND2	CTGTCTCTGATCCGCAAGCAT	GGTGGGTACATGGCAAACCTAAA
CCNE1	AAGGAGCGGGACACCATGA	ACGGTCACGTTTGCCTTCC
MYC	GGCTCCTGGCAAAGGTCA	CTGCGTAGTTGTGCTGATGT
GLI1	AGCGTGAGCCTGAATCTGTG	CAGCATGTACTGGGCTTTGAA
CDK4	TCAGCACAGTTCGTGAGGTG	GTCCATCAGCCGGACAACAT
BCL-2	GGTGGGGTCATGTGTGTGG	CGGTTTCAGGTACTCAGTCATCC
GAPDH	ATCACTGCCACCCAGAAGAC	TTTCTAGACGGCAGGTCAGG

Credit Author Statement

Maoping Cai: Carried out most of the experiments and wrote the original draft. Yaying Hong: Performed flow cytometry analysis. Songyu Li and Jiading Guo: Performed animal experiments. Yang-Zi Ren, Yuan Liu and Zhe-Sheng Chen: Reviewed and revised the article. Ninghan Feng, Zhanghui Chen and Shan-Chao Zhao: Conceived the project and designed the experiments.

Declaration of Competing Interest

The authors declare that they have no known competing financial interests or personal relationships that could have appeared to influence the work reported in this paper.

Acknowledgments

The authors gratefully acknowledge the funds from the National Key Research and Development Program, China (2023YFE0204500), National Natural Science Foundation of China (82272856 and 82370099), the Guangdong Basic and Applied

Basic Research Foundation (2022A1515010437), the President's Foundation of the Third Affiliated Hospital of Southern Medical University (No. YM2021010), Zhujiang Talent Program (2019QN01Y279) and Zhanjiang Science and Technology Project (2022A01107, 2023A21305).

References

1. Siegel RL (2022) Cancer statistics, CA Cancer J Clin, 72: 7-33.
2. Xia C (2022) Cancer statistics in China and United States, 2022: profiles, trends, and determinants. Chin Med J (Engl), 135: 584-90.
3. Liu J (2022) Prostate cancer treatment - China's perspective. Cancer Lett, 550: 415215927.
4. Cornford P (2021) EAU-EANM-ESTRO-ESUR-SIOG Guidelines on Prostate Cancer. Part II-2020 Update: Treatment of Relapsing and Metastatic Prostate Cancer. Eur Urol, 79: 263-82.
5. Jamroze A, G Chatta, DG Tang (2021) Androgen receptor (AR) heterogeneity in prostate cancer and therapy resistance. Cancer Lett, 518: 1-9.
6. Yamada Y, H Beltran (2021) The treatment landscape of metastatic prostate cancer. Cancer Lett 519: 20-9.
7. Lu, D. and Y. Gao (2022) Immune Checkpoint Inhibitor-related Endocrinopathies. J Transl Int Med, 10: 9-14.
8. Cai M (2023) Current therapy and drug resistance in metastatic castration-resistant prostate cancer. Drug Resist Updat, 68: 100962.
9. Ruiz de Porras V, A Font, A Aytes (2021) Chemotherapy in metastatic castration-resistant prostate cancer: Current scenario and future perspectives. Cancer Lett, 523:162-9.
10. Scott LJ, CM Perry, Tegaserod (1999) Drugs, 1999. 58: 491-6; discussion 497-8.
11. Hong YG (2023) The RNA m6A Reader YTHDF1 Is Required for Acute Myeloid Leukemia Progression. Cancer Res, 83: 845-60.
12. Xie X (2022) Tegaserod maleate exhibits antileukemic activity by targeting TRPM8. Biomed Pharmacother, 154: 113566.
13. Liu W (2020) Repurposing the serotonin agonist Tegaserod as an anticancer agent in melanoma: molecular mechanisms and clinical implications. J Exp Clin Cancer Res, 39: 38.
14. Wang Z (2022) Tegaserod Maleate Suppresses the Growth of Gastric Cancer In Vivo and In Vitro by Targeting MEK1/2. Cancers (Basel), 14.
15. Li X (2022) Tegaserod Maleate Inhibits Breast Cancer Progression and Enhances the Sensitivity of Immunotherapy. J Oncol, 5320421.
16. Li P (2022) ELK1-mediated YTHDF1 drives prostate cancer progression by facilitating the translation of Polo-like kinase 1 in an m6A dependent manner. Int J Biol Sci, 18: 6145-62.
17. Wang Y, P Jin, X Wang (2023) N(6)-methyladenosine regulator YTHDF1 represses the CD8 + T cell-mediated antitumor im-

- munity and ferroptosis in prostate cancer via m(6)A/PD-L1 manner. Apoptosis.
18. Chen Y, G Struhl (1996) Dual roles for patched in sequestering and transducing Hedgehog, *Cell*, 87: 553-63.
 19. Jiang J (2022) Hedgehog signaling mechanism and role in cancer. *Semin Cancer Biol*, 85: 107-22.
 20. Briscoe J, PP Thérond (2013) The mechanisms of Hedgehog signalling and its roles in development and disease. *Nat Rev Mol Cell Biol*, 14: 416-29.
 21. Datta S, MW Datta (2006) Sonic Hedgehog signaling in advanced prostate cancer. *Cell Mol Life Sci*, 63: 435-48.
 22. Yu, YZ (2022) Hsa_circ_0003258 promotes prostate cancer metastasis by complexing with IGF2BP3 and sponging miR-653-5p. *Mol Cancer*, 21: 12.
 23. Xie T (2022) CircSMARCC1 facilitates tumor progression by disrupting the crosstalk between prostate cancer cells and tumor-associated macrophages via miR-1322/CCL20/CCR6 signaling. *Mol Cancer*, 21: 173.
 24. Xiao ZM (2021) SMARCC1 Suppresses Tumor Progression by Inhibiting the PI3K/AKT Signaling Pathway in Prostate Cancer. *Front Cell Dev Biol*, 9: 678967.
 25. Yan S (2023) Adipocyte YTH N(6)-methyladenosine RNA-binding protein 1 protects against obesity by promoting white adipose tissue beiging in male mice. *Nat Commun*, 14: 1379.
 26. Zhang ZW (2022) METTL3 regulates m(6)A methylation of PTCH1 and GLI2 in Sonic hedgehog signaling to promote tumor progression in SHH-medulloblastoma. *Cell Rep*, 41: 111530.
 27. Chen L (2022) O-GlcNAcylation promotes cerebellum development and medulloblastoma oncogenesis via SHH signaling. *Proc Natl Acad Sci U S A*, 119: e2202821119.
 28. Gupta P (2019) HER2-mediated GLI2 stabilization promotes anoikis resistance and metastasis of breast cancer cells. *Cancer Lett*, 442: 68-81.
 29. Jeng KS, CF Chang, SS Lin (2020) Sonic Hedgehog Signaling in Organogenesis, Tumors, and Tumor Microenvironments. *Int J Mol Sci*, 21.
 30. Kriplani P, K Guarve, Eudragit (2022) a Nifty Polymer for Anticancer Preparations: A Patent Review. *Recent Pat Anticancer Drug Discov*, 17: 92-101.
 31. Ze X, W Zou, Z Li (2021) Translational research in anti-pancreatic fibrosis drug discovery and development. *J Transl Int Med*, 9: 225-227.
 32. Hua Li, Wenyi Wei, Hongxi Xu (2022) Drug discovery is an eternal challenge for the biomedical sciences. *Acta Materia Medica*, 1: 1-3.
 33. Tulsi R (2021) Metastasis of Duodenal Adenocarcinoma to the Urinary Bladder Presenting as Hematuria. *J Transl Int Med*, 9: 143-5.